

Heat refraction and low-pressure metamorphism in the northern Flinders Ranges, South Australia

S. D. MILDREN AND M. SANDIFORD

Department of Geology and Geophysics, University of Adelaide, SA 5005, Australia.

Unusually high lateral temperature gradients associated with metamorphism of the lower sedimentary sequences of the Adelaide Fold Belt near the basal unconformity with Proterozoic gneisses of the Mt Painter Inlier in the northern Flinders Ranges raise the possibility that heat refraction can give rise to a unique type of regionally extensive, unconformity-related, contact metamorphism. Numerical models are used to explore the possibility that the metamorphism may reflect lateral variations in thermal conductivity and heat production using simple geometries appropriate to the deformed basement–cover interface at Mt Painter. The thermal models provided here show that with typical values of thermal conductivity and heat production, heat refraction can account, at most, for about 1/3 to 1/2 of the observed metamorphic signature. Additional advective heat transfer such as high-temperature fluid flow focused by the heat-refraction mechanism may have contributed to the lateral temperature gradients surrounding the basement–cover contact.

Key words: heat transfer, metamorphism, numerical modelling, thermal conductivity.

INTRODUCTION

The Mt Painter Inlier near Arkaroola in the northern Flinders Ranges of South Australia is one of the few Precambrian basement inliers within the Adelaide Geosyncline (Preiss 1987). The crystalline basement is comprised of Neoproterozoic to Mesoproterozoic gneisses (the Radium Creek Metamorphics) which have been intruded by a number of generations of granite, including an older Mesoproterozoic (Carpenterian) granite suite and a younger Ordovician (Delamerian) granite suite. Unconformably overlying the basement inlier are Upper Proterozoic to Cambrian (Adelaidean) cover sequences containing clastic and carbonate sediments and minor volcanics. In the Arkaroola region these include the Arkaroola Subgroup of the Callana Group and the overlying Burra Group (Preiss 1987).

The Mt Painter Inlier forms a structural core within the folded sediments that dip away from the basement in the range of approximately 50–70° at the contact. Deformation and metamorphism occurred during the Delamerian orogeny approximately 500 Ma ago where metamorphism resulted from anomalous thermal gradients in the Upper Proterozoic sedimentary succession surrounding the basement (Coats & Blissett 1971). This is illustrated by the cordierite-in isograd shown in Figure 1 (after mapping by G. Teale and A. Bingemer) that is located approximately 1 km from the unconformity. The occurrence of cordierite and anthophyllite in altered metabasalts and diopside in calc-silicates near the contact suggests maximum temperatures exceeded 500–550°C while cordierite-bearing metapelites imply a maximum depth of burial of about 10 km (Dymoke & Sandiford 1992). Additionally, the zone of

metasomatism evidenced by the widespread scapolitization of a variety of rock types (Coats & Blissett 1971) is similarly related to the basement–cover contact. Lateral temperature gradients in excess of 25°C km⁻¹ culminate in the amphibolite facies assemblages developed immediately above the unconformity with total lateral temperature variations in excess of 100–150°C.

Several different heat sources may have contributed to the metamorphic perturbation in this region including magmatism, heat refraction and advection of fluids. A number of granitic bodies such as the British Empire Granite were apparently intruded around the time of the metamorphism and must therefore have contributed to the thermal energy budget of this unusual terrane. However, apart from a few isolated stocks of less than 50 m diameter at the Needles and the Pinnacles, there is little correspondence between the mapped isograds and the distribution of the appropriate igneous bodies, which stands in stark contrast with the general concordance of isograds with the basement–cover unconformity. Lateral variations in the thermal conductivity of rocks, such as may be expected for a folded basement–cover unconformity (e.g. Jaupart & Provost 1985), drive the heat refraction process, possibly causing the significant change in gradient toward the basement–cover contact and providing a unique type of unconformity-related contact metamorphism. The principal aim of this paper is to examine the degree to which heat refraction may have contributed to the unique metamorphic signature of the Mt Painter region. The following section describes the results of several heat refraction models designed for this purpose. We finish with a brief discussion of some of the broader issues pertaining to heat refraction in the Australian context.

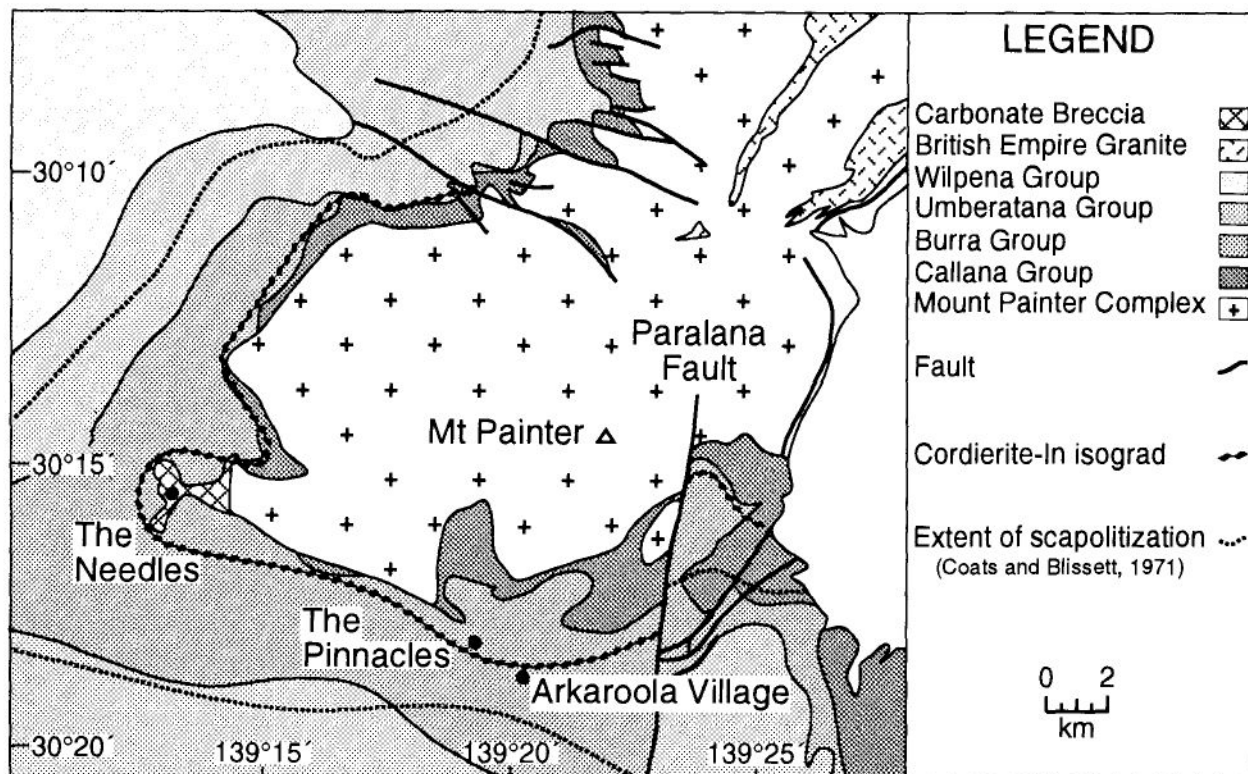


Figure 1 Map of the Mt Painter Province showing the cordierite-in isograd as mapped by G. Teale (pers. comm. 1994) and A. Bingemer (pers. comm. 1994), and the zone of scapolitization surrounding the basement.

HEAT REFRACTION AND UNCONFORMITY-RELATED CONTACT METAMORPHISM

The principal mode of heat transfer in the crust is by conduction. Since rocks of different mineral composition and porosity have significantly different conductivities, lateral variations in thermal conductivity may be expected to result from the various structural geometries produced during deformation, magmatism, diapirism etc. The process by which these geometries alter the flow of heat to create a focusing effect is known as heat refraction. The effects of heat refraction are readily illustrated with reference to an idealized body of high-conductivity rocks surrounded by lower conductivity rocks. A highly conductive core will act as a conduit for thermal energy, transferring heat at a faster rate than the surrounding poorly conductive regions (Jaupart & Provost 1985; Allen & Chamberlain 1989). The resulting focusing of thermal energy will raise the temperature above the conductive core and lower it below, relative to the same rocks at the same depths away from the core. Similarly, heat will be 'refracted' around cores of low thermal conductivity, decreasing the temperature above and increasing the temperature below the core.

In order to model the possible thermal effects of heat refraction at Mt Painter, the following constraints on the geometry and magnitude of thermal conductivity and heat production are adopted.

Geometry

We have used a simple sinusoidal geometry to simulate the deformed basement cover interface of the type

observed in the Mt Painter Province (Figure 2). The minimum amplitude and wavelength of the unconformity, determined from the regional geological constraints (e.g. Coats & Blissett 1971), are estimated at 9 km and 30 km, respectively. We note that the decoupling of structures in the cover from the basement structure may imply significantly greater effective wavelengths for the unconformity, and in the simulations described below we consider a range of wavelengths of the order of 30–60 km.

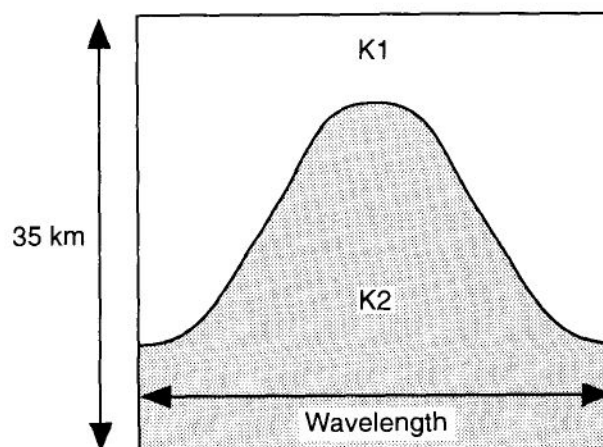


Figure 2 Basic geometry used in simulating a simple sinusoidal interface between two layers of differing conductivity.

Thermal conductivity

The thermal conductivity values used for the heat refraction models were estimated using averages of conductivity ranges for specific rock types listed in Figure 3. The Mt Painter Complex comprises predominantly gneiss, granite, granodiorite and quartzite, which gives an average thermal conductivity of around $3.5 \text{ W m}^{-1} \text{ K}^{-1}$. The Adelaidean cover sequence contains less conductive shale, conglomerate, limestone and sandstone. While the conductivity structure of this sequence is likely to be very heterogeneous at the 10–100 m-scale, we consider that on the kilometre-scale appropriate to the observed lateral variations in metamorphic grade it can be treated as a homogeneous sequence with an average conductivity appropriate to a mixture of shale, limestone and sandstone. Such an averaging suggests a thermal conductivity value significantly less than $3.0 \text{ W m}^{-1} \text{ K}^{-1}$. Moreover, prior to Delamerian metamorphism, these sediments are likely to have contained a substantial amount of formation water, and water-filled porosity significantly lowers the bulk thermal conductivity (Sugawara & Yoshizawa 1961; Woodside & Messmer 1961a,b; Brigaud & Vasseur 1989), suggesting the average thermal conductivity for the Adelaidean cover sequence prior to metamorphism may have been lower. In view of these considerations we model conductivities for the cover sequence in the range $1.5\text{--}2.5 \text{ W m}^{-1} \text{ K}^{-1}$.

It is well known that in the temperature range considered here (300–500°C), the conductivity of most rocks is inversely correlated with temperature (e.g. Clark 1966; Lerche 1991). However, because of the complexity introduced by non-linearity in numerical approximations

to the differential equations governing heat conduction, in all simulations we consider that the thermal conductivity is independent of temperature. We note that there is little evidence to suggest that the conductivity contrasts (i.e. the ratio of conductivities) between rock types change appreciably with temperature.

Heat production

The Mt Painter Inlier is well recognized for its anomalous radioactive element content (Drexal & Major 1990). Typical basement heat production values lie between 2×10^{-6} and $4 \times 10^{-6} \text{ W m}^{-3}$ and values of the Mt Painter Inlier may exceed this considerably with conservative estimates of 5 or $6 \times 10^{-6} \text{ W m}^{-3}$. The heat production of the Adelaidean cover sequence is unconstrained, so here we model a number of scenarios in which (i) the distribution of heat production is assumed to play no role (which corresponds to either zero heat production or to uniformly distributed heat production across the basement–cover interface); and (ii) heat production is assumed to be strongly concentrated in the basement.

NUMERICAL METHODS

Quantitative modelling of heat refraction effects at Mt Painter requires solutions to the steady state heat equation for cases where the thermal conductivity ($k_{x,xz}$) and heat production ($A_{x,xz}$) varies in space, such that:

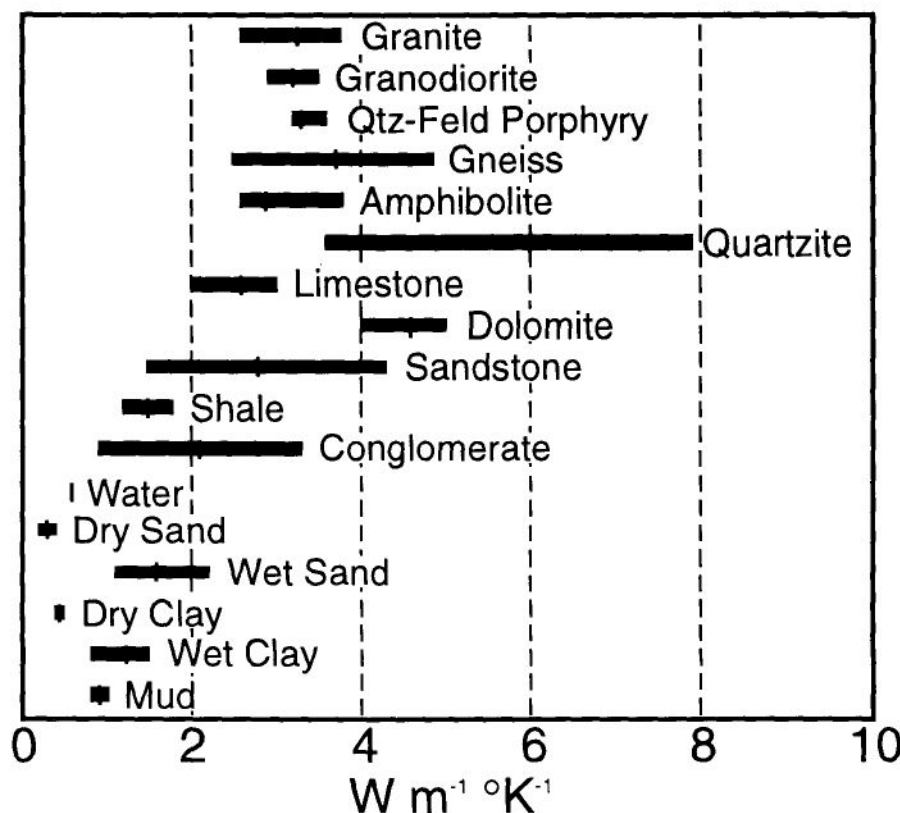


Figure 3 Range of thermal conductivities of various rock types (after Clark 1966 and Kappelmeyer & Haenel 1974). Average values are indicated by the vertical line.

$$0 = \nabla \cdot (k_{x,y,z} \nabla T) + A_{x,y,z} \quad (1)$$

where ∇ is the gradient operator ($\frac{\partial}{\partial x}, \frac{\partial}{\partial y}, \frac{\partial}{\partial z}$) and T is temperature. Of the quantitative methods available for solutions of linear differential equations, only numerical solutions allow the incorporation of relatively complex boundary conditions and spatial variations of thermal parameters appropriate to geological settings. In this study a finite difference algorithm appropriate to 2-D spatial variations in conductivity has been implemented to approximate equation (1). In the algorithm employed here, the partial differential equations are replaced by finite differences on a 2-D grid covering the solution domain and iterated until convergence to a final steady solution. We used a Gauss-Seidel finite difference method incorporating a five point difference molecule. This explicit method is slowly converging so an acceleration factor for successive over-relaxation was included in order to speed up the iteration.

In the numerical solutions, the upper boundary (surface) of the solution domain is set to a fixed temperature appropriate to the Earth's surface and the lower boundary condition at a depth of 35 km is defined at a constant temperature of 800°C. The side boundaries of the solution domain are considered to be adiabatic, that is, they have zero heat flux so they can be considered to be periodic, serving as lines of symmetry in any structure. The constant basal boundary condition is clearly somewhat artificial and serves to dictate the

overall thermal state within the solution domain. The magnitude of absolute temperatures calculated at any point within the solution domain are clearly dependent on this boundary condition, and consequently should only be considered as illustrative. In contrast, the magnitude of the lateral temperature differences and gradients are more robust to this boundary condition and thus can be awarded much greater significance.

RESULTS

We have investigated eight different thermal conductivity and heat production structures that include the range of parameters described above, with the results shown in Figures 4 to 7. Figures 4a to 4d illustrate different thermal parameters for a wavelength λ of 30 km. Figure 4a illustrates the thermal structure obtained for a basement to cover conductivity ratio of 3.5 : 1.5 with no internal heat production in the basement. Note that at 10 km depth isotherms are elevated by approximately 30°C near the basement and the maximum temperature is about 330°C. A somewhat smaller conductivity ratio of 3.5 : 2 produces even smaller temperature differences between the margin and the contact (Figure 4b). The result of applying a heat production contrast across the interface is shown in Figures 4c and 4d. Heat production in the basement augments the refraction effect to produce

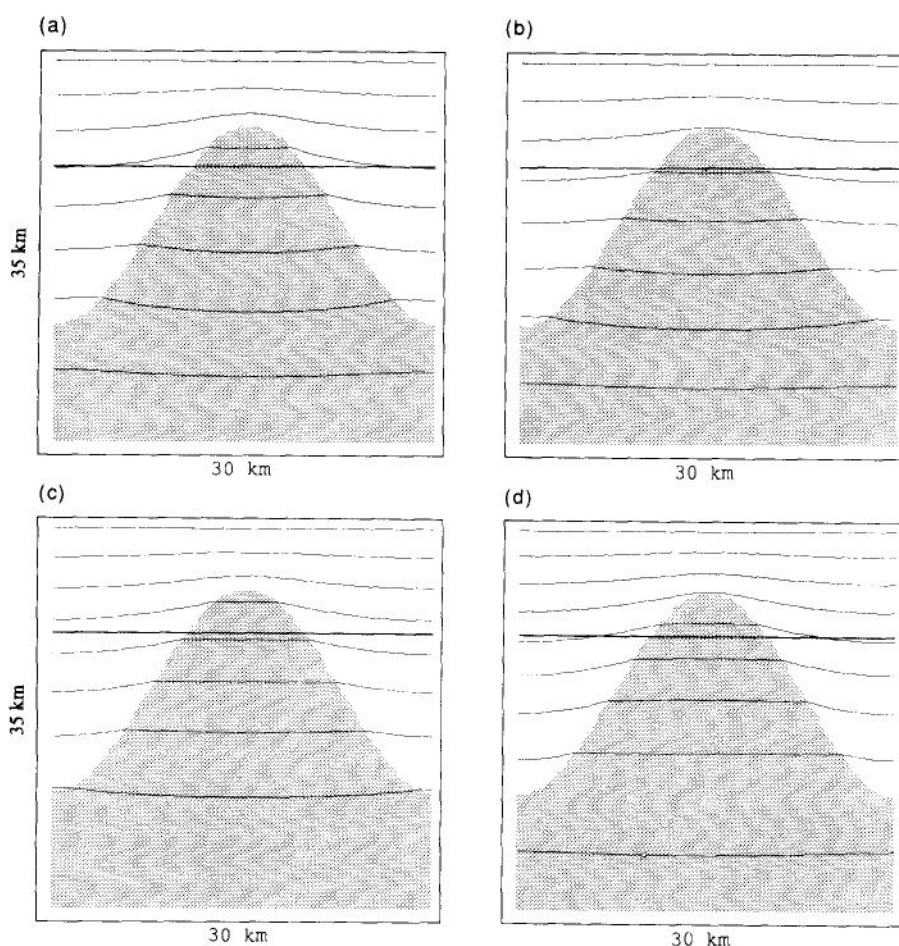


Figure 4 Selected steady-state models simulating heat refraction associated with a sinusoidal basement-cover interface appropriate to the southern Mt Painter Province with a wavelength of 30 km. The following conductivities and heat production values were used: (a) $k_{\text{cover}} = 1.5 \text{ W m}^{-1} \text{ K}^{-1}$, $k_{\text{basement}} = 3.5 \text{ W m}^{-1} \text{ K}^{-1}$, $A_{\text{cover}} = 0 \text{ W m}^{-3}$, $A_{\text{basement}} = 0 \text{ W m}^{-3}$; (b) $k_{\text{cover}} = 2.0 \text{ W m}^{-1} \text{ K}^{-1}$, $k_{\text{basement}} = 3.5 \text{ W m}^{-1} \text{ K}^{-1}$, $A_{\text{cover}} = 0 \text{ W m}^{-3}$, $A_{\text{basement}} = 0 \text{ W m}^{-3}$; (c) $k_{\text{cover}} = 2.0 \text{ W m}^{-1} \text{ K}^{-1}$, $k_{\text{basement}} = 3.5 \text{ W m}^{-1} \text{ K}^{-1}$, $A_{\text{cover}} = 0 \text{ W m}^{-3}$, $A_{\text{basement}} = 3 \times 10^{-6} \text{ W m}^{-3}$; (d) $k_{\text{cover}} = 2.0 \text{ W m}^{-1} \text{ K}^{-1}$, $k_{\text{basement}} = 3.5 \text{ W m}^{-1} \text{ K}^{-1}$, $A_{\text{cover}} = 0 \text{ W m}^{-3}$, $A_{\text{basement}} = 5 \times 10^{-6} \text{ W m}^{-3}$. Ten kilometre depth horizons are marked on each figure. Isotherms are spaced at 100°C intervals.

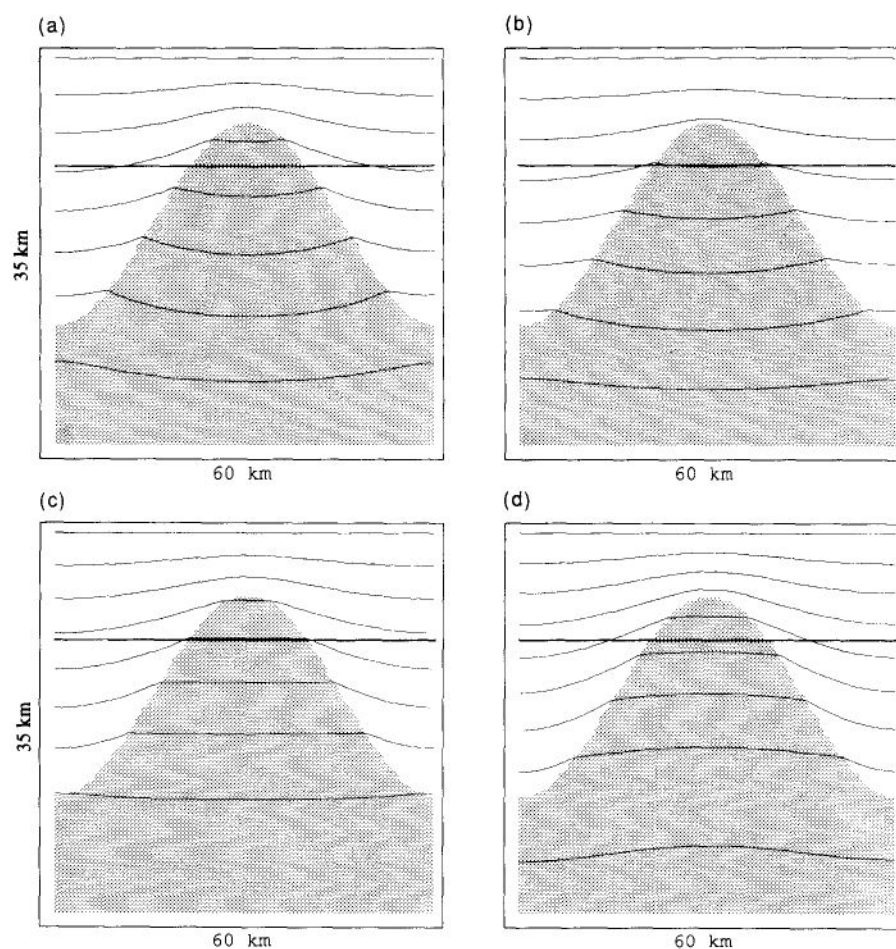


Figure 5 Selected steady-state models simulating heat refraction associated with a sinusoidal basement-cover interface appropriate to the southern Mt Painter Province with a wavelength of 60 km. Thermal parameters in Figures 5a–d correspond to Figures 4a–d. Ten kilometre depth horizons are marked on each figure. Isotherms are spaced at 100°C intervals.

lateral temperature gradients in the order of $5^{\circ}\text{C km}^{-1}$ for basement heat production of $3 \times 10^{-6} \text{ W m}^{-3}$ and $5 \times 10^{-6} \text{ W m}^{-3}$ (Figures 4c,d).

The effect of increasing the fold wavelength of the basement to 60 km is shown in Figures 5a to 5d, which use the thermal parameter set identical to Figures 4a to 4d. A comparison of the thermal regimes obtained shows a dramatic increase in the lateral temperature variation at 10 km depth. For example, the maximum temperature difference attained at 10 km depth is increased from 30 to 50°C for the cases illustrated in Figures 4a and 5a, 25 to 30°C between Figures 4b and 5b, 50 to 75°C between

Figures 4c and 5c and 50°C to 110°C between Figures 4d and 5d. Figure 5d predicts a temperature at 10 km depth of approximately 330°C at the margin of the solution domain which is raised to around 440°C at the basement–cover interface, resulting in maximum lateral temperature gradients in the order of $10\text{--}15^{\circ}\text{C km}^{-1}$. These data are summarized in Figures 6 and 7. Figure 6 illustrates the temperature profiles at 10 km, depth for each of the eight models described above for 30 and 60 km, respectively, while Figure 7 illustrates the variations in the lateral temperature gradient at 10 km depth across each model. The significance of these results and a

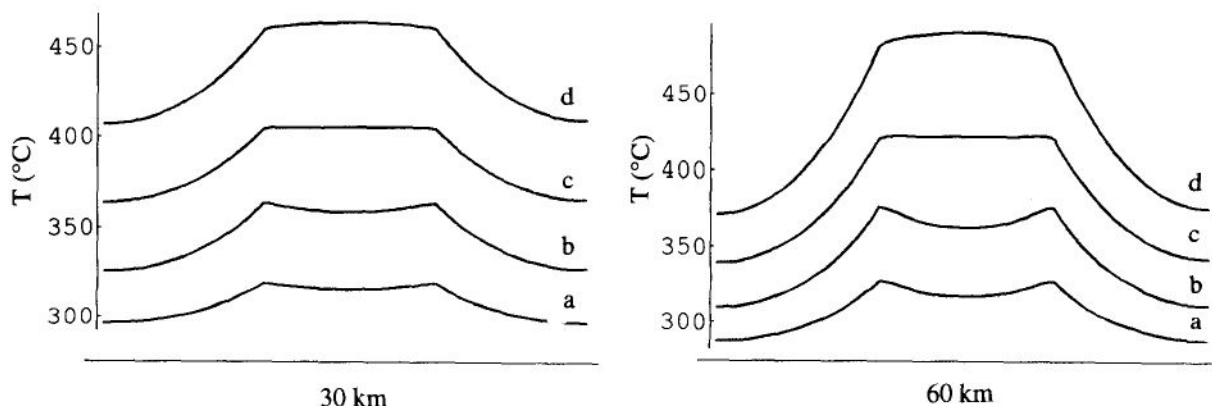


Figure 6 Temperature profiles at 10 km depth for the models shown in Figure 4 (left) and Figure 5 (right).

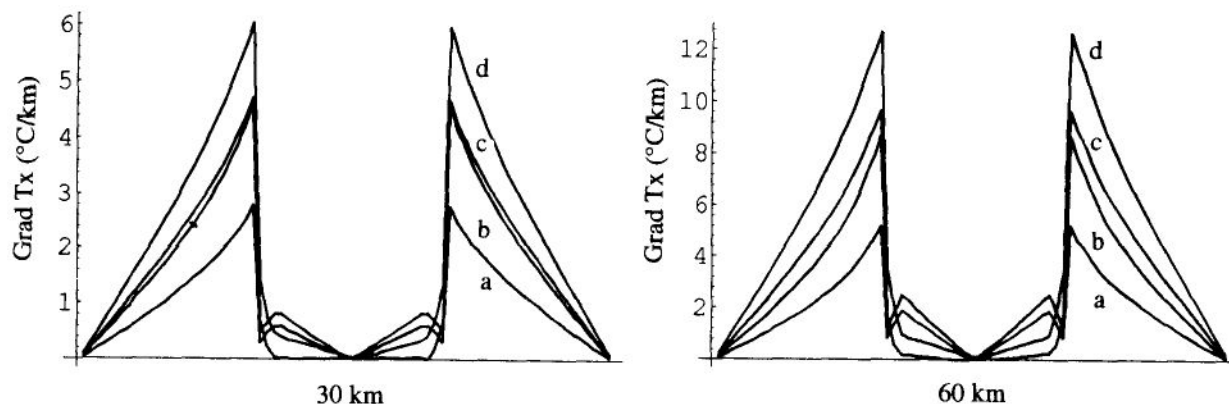


Figure 7 Horizontal temperature gradients at 10 km depth for the models shown in Figure 4 (left) and Figure 5 (right).

discussion of the evolution of the metamorphic aureole follows.

DISCUSSION

The results outlined in the previous section show that for a simple sinusoidal interface the effect of heat refraction is sensitive both to the wavelength and the conductivity ratio. Significant effects are obtained for large wavelengths and for high conductivity contrasts. However, for the most extreme geometries and thermal parameter ranges likely to apply in the Mt Painter setting, heat refraction alone cannot account for more than about 1/3 of the observed metamorphic signature. If the conductivity structure is coupled with heat production variation, as appears likely to be the case for Mt Painter, the lateral temperature variations are of the order of 100°C at a depth of 10 km. Such a variation represents in excess of half the observed temperature variation, suggesting that the heat refraction mechanism may be an important contributing factor to the unique metamorphic signature at Mt Painter.

While the calculations summarized above suggest that heat refraction alone appears to be inadequate to explain the extent of the metamorphic signature, it is conceivable that thermal loading by a heat refraction mechanism may have activated advective hydrothermal systems. It is well known that large transient temperature variations attributed to magmatic intrusions decrease local fluid density and cause fluid ascent and circulation around plutons (Furlong *et al.* 1992; Hanson 1992). Using an intrusive analogy we can infer that convective systems may be generated by thermal perturbations arising from lateral contrasts in the thermal properties of rocks. Temperature increases associated with heat refraction along the contact must result in a decrease in fluid density and thus fluid pressure in the region of the anticlinal core, inducing fluid flow towards the anticline and up temperature at depth, and then upward and down temperature in the region of heating. It is conceivable that a convective system may be established with upwelling along the sides of the fold. This pattern of flow must redistribute heat from the sides of the fold towards its top, resulting in the stretching of isotherms vertically

in the region of the interface, thus producing a temperature distribution, more congruous with the observed isograd distribution around the Mt Painter Inlier. The main point here is that although heat refraction may not be substantial enough to generate the observed effects, it may provide the thermal mechanism responsible for localizing and driving regional fluid flow which acts to augment the thermal perturbation (e.g. Smith & Chapman 1983).

Unlike an intruded magma, the 'heat refraction' source will not slowly dissipate through cooling unless the conductivity contrast is removed in some way. This fluid circulation may be maintained over long periods, providing the system is continually recharged. Preliminary oxygen isotope analysis of carbonates reveals isotopic depletion of $\delta^{18}\text{O}$ by as much as 12‰ as metamorphic grade increases towards the basement, consistent with extensive fluid infiltration focused along the basement–cover interface (A. Bingemer, pers. comm. 1994). Significant alteration of the Wooltana Volcanics in the Callana Group has been described by Foden (pers. comm. 1994), who show that there has been partial resetting of the strontium isotopic system and pervasive potassium metasomatism, both of which require large pervasive fluid fluxes. Widespread, structurally controlled Cu-mineralization in the carbonates of the Callana Group (Coats & Blisset 1971) may well correlate with this metasomatic activity. As suggested above heat refraction as a result of lateral variations in conductive properties between rock types may provide the driving mechanism for fluid flow within the lowermost units of the Adelaidean cover sequence in the Mt Painter region, with several sources responsible for supplying the hydrothermal fluid at different times. Fluids are most likely to be derived from the Adelaidean sediments undergoing compaction and probable metamorphism during Delamerian deformation.

Finally, it is worth speculating on some of the broader issues raised by our analysis of the unusual metamorphic signature at Mt Painter in terms of heat refraction. Elsewhere in the Adelaide Fold Belt there are significant structural culminations and while they rarely expose basement, the possibility that the basement is structurally elevated beneath these regions may allow a significant heat refraction effect. If, as we suggest for the Mt Painter

Region, heat refraction is important in localizing and driving hydrothermal systems, then these structural culminations located above elevated, hot basement may be regions of enhanced hydrothermal activity, which could well make them prospective targets for economic mineralization. Many of the central Australian intracratonic basins, such as the Cooper Basin, must now overlie a complex basement structure with thermal properties resembling the northern Flinders Ranges. The potential heat refraction in the basement may significantly mediate the heat flow into the overlying insulating succession and potentially give rise to very marked lateral temperature variations. Such lateral variations in thermal structure may have important ramifications for understanding spatial variations in maturation in these basins.

ACKNOWLEDGEMENTS

This work was completed as part of a BSc(Hons) thesis (SM) undertaken as part of a broader study of the hydrothermal evolution of the Mt Painter Inlier organized by MS. We acknowledge the important contributions of all other participants in this ongoing study and especially the generosity afforded by the Sprigg family during our field studies in the Arkaroola region. We thank Annette Bingemer and Graeme Teale for many discussions concerning metamorphism in the Mt Painter region, and for providing the information concerning the distribution of isograds shown in Figure 1. Nick Oliver is thanked for comments on an earlier version of this manuscript.

REFERENCES

- ALLEN T. & CHAMBERLAIN C. P. 1989. Thermal consequences of mantled gneiss dome emplacement. *Earth and Planetary Science Letters* **93**, 392–404.
- BRIGAUD F. & VASSEUR G. 1989. Mineralogy, porosity and fluid control on thermal conductivity of sedimentary rocks. *Geophysical Journal* **98**, 525–542.
- CLARK S. P. 1966. Thermal conductivity. In Clark S. P. ed. *Handbook of Physical Constants*, pp. 459–481. Geological Society of America Memoir 97.
- COATS R. P. & BLISSET A. H. 1971. Regional and economic geology of the Mount Painter Province. *Geological Survey of South Australia Bulletin* **43**.
- DREXAL J. F. & MAJOR R. B. 1990. Mount Painter uranium and rare earth deposits. In Hughes F. E. ed. *Geology of the Mineral Deposits of Australia and Papua New Guinea*, pp. 993–998. The Australasian Institute of Mining and Metallurgy, Melbourne.
- DYMOKE P. & SANDIFORD M. 1992. Phase relationships in Buchan facies series pelitic assemblages: calculations with application to andalusite–staurolite paragenesis in the Mount Lofty Ranges, South Australia. *Contributions to Mineralogy and Petrology* **110**, 121–132.
- FURLONG K. P., HANSON R. B. & BOWERS J. R. 1992. Modelling thermal regimes. In Kerrick D. M. ed. *Contact Metamorphism*, **26** pp. 437–505. Mineralogical Society of America, Reviews in Mineralogy.
- HANSON R. B. 1992. Effects of fluid production on fluid flow during regional and contact metamorphism. *Journal of Metamorphic Geology* **10**, 87–97.
- JAGPART C. & PROVOST A. 1985. Heat focusing, granite genesis and inverted metamorphic gradients in continental collision zones. *Earth and Planetary Science Letters* **73**, 385–397.
- KAPPELMAYER O. & HAENEL R. 1974. *Geothermics: with Special Reference to Applications*. Geoexploration Monographs 1. Borntraeger, Berlin.
- LERCHE I. 1991. Temperature dependence of thermal conductivity and its impact on assessments of heat flux. *Pageoph* **136**, 191–200.
- PREISS W. V. 1987. The Adelaide Geosyncline: Late Proterozoic stratigraphy, sedimentation, palaeontology and tectonics. *Geological Survey of South Australia Bulletin* **53**, 34–41.
- SMITH L. & CHAPMAN D. S. 1983. On the thermal effects of groundwater flow: 1. Regional systems. *Journal of Geophysical Research* **88**, 593–608.
- SUGAWARA A. & YOSHIZAWA Y. 1961. An investigation on the thermal conductivity of porous materials and its application to porous rock. *Australian Journal of Physics* **14**, 468–480.
- WOODSIDE W. & MESSMER J. H. 1961a. Thermal conductivity of porous media I. Unconsolidated sands. *Journal of Applied Physics* **32**, 1688–1698.
- WOODSIDE W. & MESSMER J. H. 1961b. Thermal conductivity of porous media II. Consolidated rocks. *Journal of Applied Physics* **32**, 1699–1706.

(Received 1 December 1993; accepted 14 January 1995)